Inorganic Chemistry

pubs.acs.org/IC Article

Distorted Copper(II) Complex with Unusually Short CF···Cu Distances

Claire C. Cody,[§] H. Ray Kelly,[§] Brandon Q. Mercado, Victor S. Batista,* Robert H. Crabtree,* and Gary W. Brudvig*

Cite This: *Inorg. Chem.* 2021, 60, 14759−14764 Read Online

ACCESS | Metrics & More | Article Recommendations | Supporting Information

ABSTRACT: We find a Cu(II)-(**L-CF$_3$**)$_2$ complex (**L-CF$_3$** = 2,2,2-trifluoro-*N*-[2-(pyridin-2-yl)propan-2-yl]acetamide) with a distorted "seesaw" geometry. It has the shortest crystallographic CF···Cu distances yet reported, to the best of our knowledge (<2.6 Å), for which computational and experimental data indicate a secondary bonding interaction. A comparison with a CCl$_3$ version and one without ligand backbone *gem*-dimethyl groups suggests a steric origin for the distorted geometry, resulting from the specific ligand interactions.

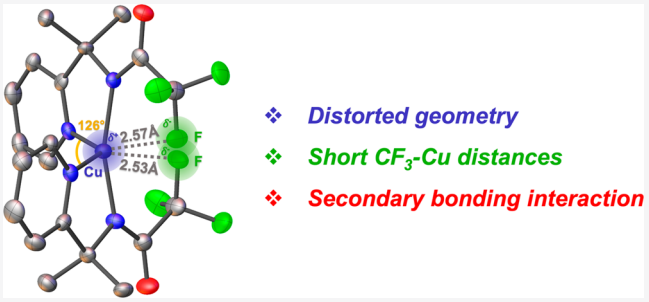

Fluorocarbon C−F bonds are normally noncoordinating,[1] with few C−F···M (M = transition metal) interactions being known, especially for late first-row transition metals.[1−3] C−F···M interactions may model early stages of C−F activation, and M···F interactions may also influence some catalytic systems.[4,5] CF$_3$ groups are often incorporated into ligands in order to tune their electronic character,[6] in which case secondary M···F interactions can result,[7] but the M···F interaction itself has been less studied.

Attempts have been made over the years to qualify M···F interactions, particularly in solid-state crystal structures. The general understanding is that this type of "secondary binding" involves distances intermediate to the sums of the covalent radii and van der Waals radii of the metal and fluorine atoms. However, van der Waals radii can be somewhat arbitrary, and a seminal review of M−F interactions by Plenio proposed that an interaction <2.7 Å for first-row transition-metal complexes is a reasonable threshold.[8] A survey of the Cambridge Structural Database (updated November 2020) returned only six structures with a Cu···F contact to CF$_3$ groups of <2.7 Å. Only two of those structures had a Cu···F contact of <2.6 Å, neither of which had N-donor ligand environments.[9,10]

While attempting to tune the electronic effects of a series of Cu complexes for water oxidation catalysis,[11] we came across an unusual coordination environment of a distorted seesaw Cu(II)-(**L-CF$_3$**)$_2$ complex (**L-CF$_3$** = 2,2,2-trifluoro-*N*-[2-(pyridin-2-yl)propan-2-yl]acetamide) with short Cu···F distances. We now report its synthesis and structure and a computational analysis of the nature of the Cu···F interaction. Modifications of the complex include a CCl$_3$ version and one without ligand backbone *gem*-dimethyl groups, in order to investigate electronic and steric factors contributing to the close Cu···X distance as well as to the distorted geometries.

While a seesaw geometry is uncommon for Cu(II), it is not unprecedented. Cu(II) coordination complexes can be four-, five-, or six-coordinate and can adopt a range of different geometries. Due to its d^9 electron configuration giving rise to a classic Jahn−Teller distortion, Cu(II) tends to form complexes that are square planar or octahedral with axial elongation, yet tetrahedral distortions are quite common.[12] In a number of cases, interligand steric repulsion leads to a distorted geometry.[13,14] However, the combination of a distorted geometry and close M···F contacts has not been reported so far; in other cases, M···F contacts are axial, allowing the conventional (N, O) donor ligands to adopt a square-planar geometry.[15,16]

SYNTHESIS AND CHARACTERIZATION

The ligand **L-CF$_3$** was synthesized by coupling a commercially available primary amine with trifluoroacetic anhydride. The copper complex **1** was then generated by adding 2 equiv of **L-CF$_3$** to Cu(OAc)$_2$·H$_2$O in an acetonitrile/methanol mix (9/1 v/v) (Scheme 1). Single crystals for X-ray diffraction were grown by slow diffusion of pentane into a dichloromethane solution of **1**. The absence of counterions in the crystal structure indicates that the amide ligands are deprotonated, no

Received: June 30, 2021
Published: September 21, 2021

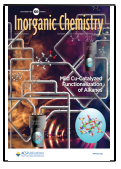

https://doi.org/10.1021/acs.inorgchem.1c01958
Inorg. Chem. 2021, 60, 14759−14764

Scheme 1. Synthetic Scheme of 1 (X = F) and 2 (X = Cl)

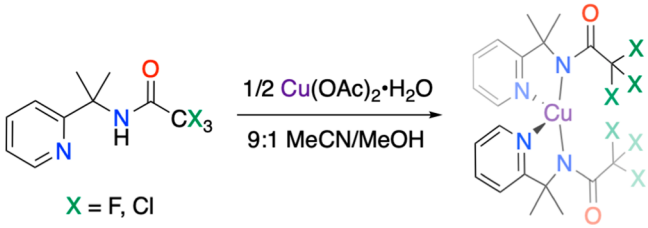

doubt by the acetate ions present in the synthesis. ATR-FTIR spectra show a shift in the amide C═O stretching frequency from 1716.4 cm^{-1} in the free ligand to 1639.2 cm^{-1} in the complex (Figure S4), consistent with ligand coordination to the Cu center. The color of **1** results from a λ_{max} band at 643 nm with $\varepsilon \approx 130$ M^{-1} cm^{-1}, consistent with a Cu d−d transition (Figure S6).

The crystal structure of **1** shows a bis-ligated Cu center cocrystallized with two dichloromethane solvent molecules (Figure 1). Key bond lengths and angles can be found in Table 1. The Cu···F distances are 2.569 and 2.530 Å, intermediate between the sum of the covalent radii[17] (1.32 + 0.57 = 1.89 Å) and of the van der Waals radii[18] (1.4 + 1.47 = 2.9 Å) and significantly shorter than Plenio's[8] suggestion that 2.7 Å is typical for such a secondary interaction.

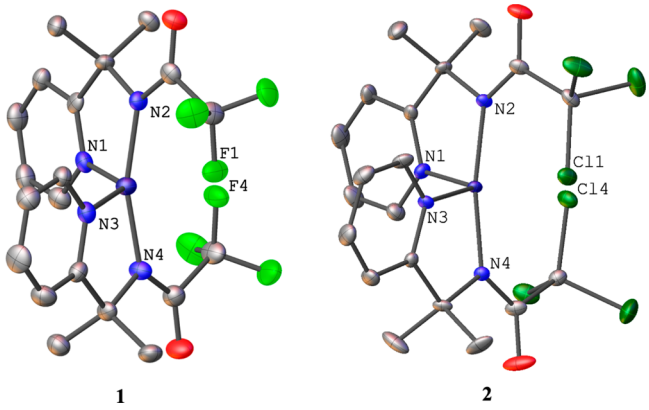

Figure 1. Single-crystal X-ray structures of **1** and **2**, with 50% thermal ellipsoid probability levels. Hydrogen atoms and solvent molecules are omitted for clarity.

Table 1. Selected Bond Lengths (Å), Distances (Å), and Angles (deg) for 1 and 2

	1	2
Cu−N1 (py)	2.003(5)	2.049(3)
Cu−N2 (amide)	1.930(4)	1.947(3)
Cu−N3 (py)	1.999(4)	2.047(3)
Cu−N4 (amide)	1.913(4)	1.939(3)
Cu···X1	2.569	2.708
Cu···X4	2.530	2.707
N1−Cu−N2	83.71(18)	83.87(13)
N3−Cu−N4	83.39(18)	83.21(13)
N1−Cu−N3	125.88(18)	112.20(13)
N2−Cu−N4	162.45(18)	169.33(14)

Further information was obtained by electron paramagnetic resonance (EPR) spectroscopy and electrochemical methods. X-band continuous wave EPR spectroscopy of **1** displayed a rhombic spectrum with $g_x = 2.029$, $g_y = 2.099$, and $g_z = 2.241$ with Cu hyperfine splittings of 331, 0, and 222 MHz (Figure S7 and Table S1). The g_z value is known to be indicative of the tetrahedral distortion of four-coordinate Cu(II) complexes, with g_z values of less than 2.20 for square-planar complexes and close to 2.40 for tetrahedral complexes.[19] This is due to mixing of the d_{z^2} orbital into the singly occupied $d_{x^2-y^2}$ orbital. A g_z value of 2.241 for **1** suggests that the distorted geometry observed in the crystal structure is maintained in solution. An oxidative sweep in a cyclic voltammogram up to 1.5 V vs Fc/Fc^+ (Fc = ferrocene) showed no features above background, indicating that the complex is not easily oxidized. A scan in the reductive direction showed a quasi-reversible feature with $E_{1/2} = -1.00$ V vs Fc/Fc^+ (Figure S8). The electrochemical and EPR data together characterize the metal center as a distorted Cu(II), $S = 1/2$ complex.

In order to test the generality, we attempted to synthesize the CCl_3 version (**2**) by an analogous method (Scheme 1); however, we were only able to recover unreacted starting material. Thinking that this was due to the lower stability of the complex disfavoring the reaction, likely related to a difference in pK_a values of the CCl_3 versus the CF_3 ligand, we scanned a number of different bases in the reaction, including K_2CO_3, KOH, and excess NaOAc. While we were unable to obtain a large enough quantity of material for bulk analysis, upon adding KOH we were able to isolate a few teal-colored crystals that showed a similar distorted structure by single-crystal X-ray diffraction (Figure 1). For complex **2**, the Cu···Cl distances are 2.708 and 2.707 Å, which are longer than the analogous Cu···F distances due to the larger size of the Cl atoms. These distances are still intermediate between the sum of the covalent radii[17] (1.32 + 1.02 = 2.34 Å) and of the van der Waals radii[18] (1.4 + 1.77 = 3.2 Å), and in fact the effective distance is shorter for the Cl version; the difference in atomic size between F and Cl is ∼0.4 Å, while the difference in the Cu···X distances is only ∼0.2 Å. The slightly longer Cu−N bond lengths in complex **2**, together with the contraction of the effective Cu−X distances, indicate an expansion of the first coordination sphere that may be related to the lower stability of the complex.

■ ANALYSIS OF CU···F INTERACTIONS

Paramagnetism precluded us from using variable-temperature NMR to determine bond rotation barriers for the CF_3 groups or from obtaining relevant coupling constants, as has been done previously.[3,20,21] We therefore turned to density functional theory (DFT) calculations to characterize the close Cu···F contacts in **1** and to determine the origin of the unusual seesaw coordination geometry. Geometry optimizations were performed in the gas phase with the B3LYP functional[22,23] and 6-31+G(d,p) basis set[24−28] as implemented in Gaussian 16, Revision C.01,[29] and showed excellent agreement with the experimental bond distances and angles (Table S2). Single-point calculations were performed with the B3LYP functional and 6-311+(2df,p) basis set[30−35] in the solvation model based on density (SMD) continuum model for dichloromethane[36] (see the Supporting Information for detailed computational methods, comparisons with other functionals and basis sets, control calculations with dispersion correction, and benchmarking with experimental observables).

https://doi.org/10.1021/acs.inorgchem.1c01958
Inorg. Chem. 2021, 60, 14759−14764

We first characterized the strength of the short Cu···F interaction by determining the free energy barrier for the rotation of the CF_3 group in **1**. The barrier of 2.0 kcal/mol is indicative of secondary coordination rather than a true Cu−F covalency. A natural bond orbital (NBO) analysis[37,38] gave further insights. The NBO method transforms canonical molecular orbitals into localized one- and two-center orbitals that correspond to lone pairs and bonds in the Lewis structure picture. If the Cu···F interaction were truly a bonding interaction, one would expect to see a two-center NBO across the Cu−F bond. However, no such orbitals were found, and the electrons on Cu and F remained localized in one-center lone pair NBOs (Figure 2A and Figure S10). Along with the relatively small barrier for CF_3 rotation, this is consistent with the short Cu···F distance being a secondary interaction. Analogous results were obtained for the Cu···Cl interaction in **2**; the free energy barrier for CCl_3 rotation was slightly larger (6.1 kcal/mol), but no two-center NBOs were observed between Cu and Cl (Figure 2B and Figure S11). In both cases, the *p* orbitals on the halogen atom were polarized by their interactions with the Cu center, with this effect being more pronounced for the Cl orbitals of **2**. For both **1** and **2**, the unpaired electron was localized in the d_{xy} orbital of the Cu center, as indicated by the NBO analysis (Figures S10 and S11) and spin populations (Figure S12 and Table S13).

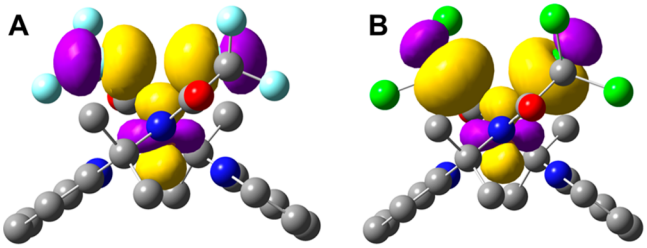

Figure 2. Three NBOs of (A) **1** and (B) **2**. The p orbitals of F/Cl and the d orbitals of Cu are localized in one-center NBOs, suggesting a secondary coordination interaction.

The quantum theory of atoms in molecules (QTAIM)[39] as implemented in Multiwfn, version 3.7,[40] was used to further analyze the Cu···X interactions in **1** and **2**. QTAIM uses the topology of the electron density ($\rho(r)$) to identify basins (atoms) and bond critical points (BCPs). Basins correspond to local maxima in $\rho(r)$, while BCPs are saddle points between two basins at which $\rho(r)$ is at a minimum in the direction of the bond and a maximum in the other directions. An analysis of the BCPs between Cu and F/Cl further supported their characterization as secondary coordination interactions (Table 2). The Laplacian of the electron density ($\nabla^2\rho(r)$) provides insight into the accumulation or depletion of $\rho(r)$ at the BCP. For both Cu···X interactions, positive values of $\nabla^2\rho(r)$ indicated a depletion of electron density at the BCP characteristic of a closed-shell interaction. The energy density ($H(r)$), composed of the potential ($V(r)$) and kinetic ($G(r)$) energy densities, at the BCP is negative in sign and small in magnitude for both interactions, which is consistent with a weak coordination interaction.[41] Finally, the delocalization index (DI) was computed between each pair of atomic basins. The DI is closely related to bond order,[42] and these small DI values indicate that there is only minor electron delocalization between the Cu center and F/Cl ligands. The magnitudes of $\rho(r)$, $H(r)$, and DI are similar but larger for Cu···Cl in comparison to Cu···F, consistent with rotation barrier and NBO analyses that showed a stronger Cu···Cl interaction. Overall, the QTAIM analysis provides additional evidence that Cu and F/Cl form secondary coordination interactions in **1** and **2**.

STERIC EFFECTS AND GEOMETRY

Cu(II) d^9 complexes tend to prefer a square-planar or octahedral geometry with elongated axial M−L bonds due to a classic Jahn−Teller distortion. However, a rich variety of Cu complex geometries exist, and **1** shows a distorted-seesaw-like geometry with a τ parameter of $\tau_4 = 0.51$ ($\tau_4 = 1.00$ for a tetrahedral geometry and $\tau_4 = 0.00$ for a square-planar geometry).[43] A possible origin of the distortion is a pseudo-*cis* Jahn−Teller effect on an elongated trigonal prism as discussed in the literature.[44] However, the geometry of our complexes more closely resembles octahedral than trigonal prismatic; thus, we primarily considered three possible causes for the distortion by experimental and computational methods: the Cu···F interaction, steric interactions between the two **L-CF_3** ligands, and the steric effects of the *gem*-dimethyl group in the backbone of **L-CF_3**.

While steric interactions between the two ligands play a large role in both the distorted geometry and the close Cu···X distances, we also wanted to investigate the steric role of the *gem*-dimethyl groups on the ligand to see whether they contributed to fixing the conformation of the amide group. When the *gem*-dimethyl group of the ligand was experimentally replaced with CH_2, the structure of the Cu complex became dependent on which Cu salt was used in the synthesis. With $Cu(OAc)_2$ as the Cu source in the same synthetic procedure as for complex **1**, the $Cu_2(OAc)_4$ paddlewheel geometry was found, with the pyridine moiety of the ligand coordinating axially and the amide twisted away due to the greater flexibility of the CH_2 moiety (Scheme 2). This paddlewheel complex (**3**) was isolated in high yield as the only product. The ligand also remained protonated, though we were unsure if this was due to a difference in the ligand pK_a in comparison to that of the dimethyl version or the fact that the more flexible ligand is less able to coordinate to the metal (metal coordination facilitates ligand deprotonation). We screened a variety of bases, including K_2CO_3, KOH, and excess NaOAc, to no avail, obtaining either Cu salts with no ligands coordinated or an unknown, insoluble brown precipitate. With $CuCl_2$ as the starting material, structure **4**, analogous to **1**, was adopted (Scheme 2). Since Cl^- counterions are not basic like acetate ions, the synthesis required the addition of a base (KOH) to deprotonate the amide ligands.

Table 2. QTAIM Parameters (au) for the Cu···F and Cu···Cl Interactions in 1 and 2

atom pair	$\rho(r)$	$\nabla^2\rho(r)$	$V(r)$	$G(r)$	$H(r)$	DI
Cu···F	0.0189	0.0725	−0.0200	0.0191	−0.0010	0.0783
Cu···Cl	0.0253	0.0701	−0.0239	0.0207	−0.0032	0.1607

https://doi.org/10.1021/acs.inorgchem.1c01958
Inorg. Chem. 2021, 60, 14759−14764

Scheme 2. Synthesis of CH_2 Version *via* $Cu(OAc)_2$ (3) or $CuCl_2$ (4), Showing the Single Crystal X-ray Structures with 50% Thermal Ellipsoid Probability Levels[a]

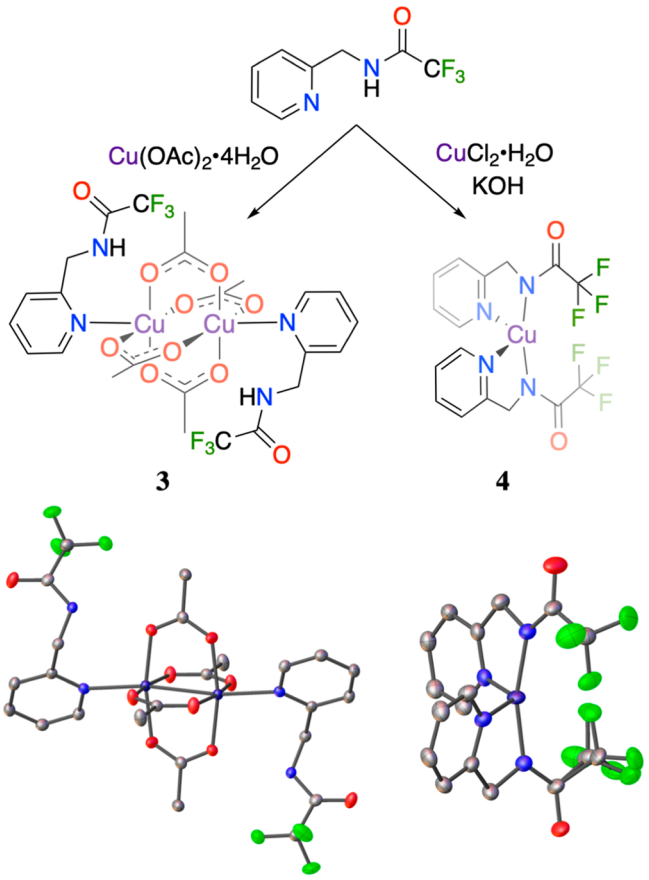

[a]Hydrogen atoms are omitted for clarity. The crystal structure for **4** displays a $-CF_3$ group disordered over two positions (see the Supporting Information for crystallographic details).

Since **4** has a geometry analogous to that of **1**, we find that the *gem*-dimethyl groups in **1** do not play a significant steric role in the distortion. In the crystal structure, one of the CF_3 groups is disordered over two positions but remarkably does not show an ~60° rotation around the C−C bond, as is typical for disordered CF_3 groups. This serves to highlight that the Cu···F interaction is weak but is significant enough to influence the CF_3 group, as the F closest to the Cu shows the most positional similarity between the two disordered positions. The Cu···F distances are slightly longer in complex **4** than in complex **1**, at 2.690 and 2.614/2.559 Å (for the disordered group). The DFT-computed CF_3 rotation barrier was 0.2 kcal/mol, substantially less than that with the *gem*-dimethyl linker (2.0 kcal/mol).

DFT calculations were also used to investigate the origin of the unusual coordination geometry of **1**. Since we have shown that the *gem*-dimethyl group in **1** has no major influence, our computational analysis focused on the relative importance of the Cu···F interaction and interligand steric effects. In addition to **1** and **2**, we considered the acetamide and formamide analogues, although these could not be synthesized. Crystallographic data from synthetic attempts for the formamide analogue indicated that the amide had hydrolyzed with loss of the formyl group so that we isolated a bidentate amine complex. Synthesis of the acetamide version provided a blue solid that was not soluble in any conventionally used solvents. We hypothesize this is because it formed an insoluble coordination polymer by coordinating to another Cu ion via the oxygen of the amide. Despite the synthetic difficulties, the acetamide and formamide versions serve as useful computational models for isolating the effect of interligand sterics on the coordination geometry. The CH_3 substituent of the acetamide version reduces the secondary coordination effect seen in **1** and **2** (the barrier for CH_3 rotation is 1.2 kcal/mol) while maintaining most of the sterics. The formamide analogue eliminates both the interactions with Cu and the substituent sterics, isolating the contribution of the interligand sterics to the molecular geometry.

Unsurprisingly, the geometries of the two model complexes were quite similar to those of **1** and **2** (Figure 3 and Table 3),

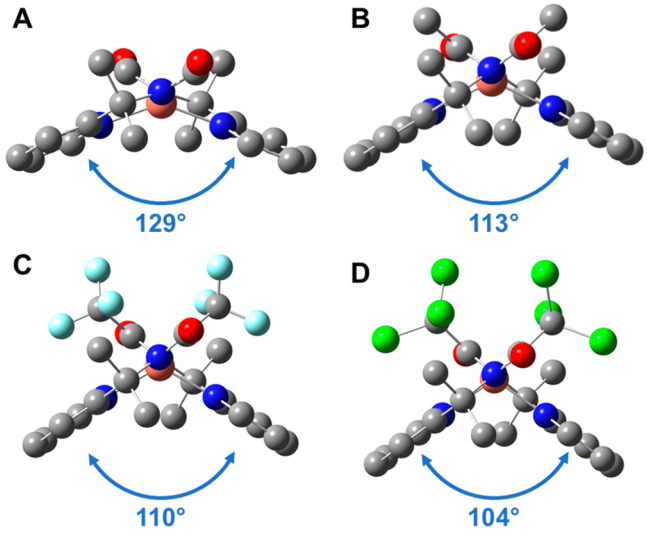

Figure 3. DFT-optimized structures of (A) the formamide analogue, (B) the acetamide analogue, (C) **1**, and (D) **2**. Hydrogen atoms are omitted for clarity. The obtuse angle between the least-squares planes of the two planar ligand domains is indicated.

showing that the weak Cu···X interactions are a consequence of the distortions, not their cause. This suggests that interligand sterics play a critical role in the distortion from a square-planar structure. As the size of the R group on the amine is increased (H < CH_3 < CF_3 < CCl_3), the overall geometry of the molecule becomes more distorted from a square-planar structure (Figure 3). With increasing size of the R group, the N−Cu−N angle between the pyridine groups gets progressively smaller to approach an ideal seesaw geometry of 90° (141° → 129° → 122° → 111°; Table 3) and the N−Cu−N angle between the amide groups increases to approach the ideal seesaw geometry of 180° (159° → 161° → 164° → 171°; Table 3). In summary, interligand steric effects and the resulting secondary interactions between F/Cl and Cu work in tandem to produce this unusual Cu(II) geometry. Steric interactions between the ligands preclude the formation of a square-planar complex even in the formamide analogue, but in the absence of secondary effects and sterically bulky R groups the angle between the pyridine rings (141°) is far from an ideal seesaw geometry (90°). Stabilizing interactions between the halogens and Cu center and the steric bulk may allow the complex to approach a true seesaw geometry.

https://doi.org/10.1021/acs.inorgchem.1c01958
Inorg. Chem. 2021, 60, 14759−14764

Table 3. Selected Calculated Bond Angles (deg) and Lengths (Å) for CuL_2 Analogues with Substituents R on the Amide Groups

R	Cu−N (py)	Cu−N (amide)	N−Cu−N (py)	N−Cu−N (amide)
H	2.04	1.93	141	159
CH_2	2.05	1.93	129	161
CF_3	2.06	1.95	122	164
CCl_3	2.09	1.97	111	171

CONCLUSIONS

We report a structure with the shortest known CF···Cu crystallographic distances. From our computational analysis, this Cu···F interaction is weak; thus, steric effects seem to be the predominant reason for the geometric distortion. These complexes demonstrate how the incorporation of various substituents for electronic tuning can also have a great and unexpected influence on the structure.

ASSOCIATED CONTENT

Supporting Information

The Supporting Information is available free of charge at https://pubs.acs.org/doi/10.1021/acs.inorgchem.1c01958.

Experimental details, additional figures and tables, computational details, and DFT coordinates (PDF)

Accession Codes

CCDC 2082885−2082888 contain the supplementary crystallographic data for this paper. These data can be obtained free of charge via www.ccdc.cam.ac.uk/data_request/cif, or by emailing data_request@ccdc.cam.ac.uk, or by contacting The Cambridge Crystallographic Data Centre, 12 Union Road, Cambridge CB2 1EZ, UK; fax: +44 1223 336033.

AUTHOR INFORMATION

Corresponding Authors

Victor S. Batista − *Department of Chemistry, and Yale Energy Sciences Institute, Yale University, New Haven, Connecticut 06520-8107, United States;* orcid.org/0000-0002-3262-1237; Email: victor.batista@yale.edu

Robert H. Crabtree − *Department of Chemistry, and Yale Energy Sciences Institute, Yale University, New Haven, Connecticut 06520-8107, United States;* orcid.org/0000-0002-6639-8707; Email: robert.crabtree@yale.edu

Gary W. Brudvig − *Department of Chemistry, and Yale Energy Sciences Institute, Yale University, New Haven, Connecticut 06520-8107, United States;* orcid.org/0000-0002-7040-1892; Email: gary.brudvig@yale.edu

Authors

Claire C. Cody − *Department of Chemistry, and Yale Energy Sciences Institute, Yale University, New Haven, Connecticut 06520-8107, United States;* orcid.org/0000-0002-9745-7087

H. Ray Kelly − *Department of Chemistry, and Yale Energy Sciences Institute, Yale University, New Haven, Connecticut 06520-8107, United States;* orcid.org/0000-0003-3811-0662

Brandon Q. Mercado − *Department of Chemistry, Yale University, New Haven, Connecticut 06520-8107, United States*

Complete contact information is available at: https://pubs.acs.org/10.1021/acs.inorgchem.1c01958

Author Contributions

[§]C.C.C. and H.R.K. contributed equally.

Notes

The authors declare no competing financial interest.

ACKNOWLEDGMENTS

This work was supported by the U.S. Department of Energy, Chemical Sciences, Geosciences, and Biosciences Division, Office of Basic Energy Sciences, Office of Science (Grant DE-FG02-07ER15909). Additional support was provided by a generous donation from the TomKat Charitable Trust. C.C.C. acknowledges support by the National Science Foundation Graduate Research Fellowship Program under Grant No. DGE-1650114. We thank the Chemical and Biochemical Instrumentation Center, particularly Dr. Fabian Menges for assistance with HRMS, and Reagan Hooper for assistance with EPR spectroscopy. V.S.B. acknowledges high-performance computing time from the Yale Center for Research Computing.

REFERENCES

(1) Kiplinger, J. L.; Richmond, T. G.; Osterberg, C. E. Activation of Carbon-Fluorine Bonds by Metal Complexes. *Chem. Rev.* **1994**, *94*, 373−431.

(2) Kulawiec, R. J.; Crabtree, R. H. Coordination Chemistry of Halocarbons. *Coord. Chem. Rev.* **1990**, *99*, 89−115.

(3) Emerson-King, J.; Prokes, I.; Chaplin, A. B. Rhodium(III) Complexes Featuring Coordinated CF_3 Appendages. *Chem. - Eur. J.* **2019**, *25*, 6317−6319.

(4) Ritter, T.; Day, M. W.; Grubbs, R. H. Rate Acceleration in Olefin Metathesis through a Fluorine-Ruthenium Interaction. *J. Am. Chem. Soc.* **2006**, *128*, 11768−11769.

(5) Rufino-Felipe, E.; Valdés, H.; Germán-Acacio, J. M.; Reyes-Márquez, V.; Morales-Morales, D. Fluorinated N-Heterocyclic Carbene Complexes. Applications in Catalysis. *J. Organomet. Chem.* **2020**, *921*, 121364.

(6) Shaffer, D. W.; Xie, Y.; Szalda, D. J.; Concepcion, J. J. Manipulating the Rate-Limiting Step in Water Oxidation Catalysis by Ruthenium Bipyridine-Dicarboxylate Complexes. *Inorg. Chem.* **2016**, *55*, 12024−12035.

(7) Popeney, C. S.; Rheingold, A. L.; Guan, Z. Nickel(II) and Palladium(II) Polymerization Catalysts Bearing a Fluorinated Cyclophane Ligand: Stabilization of the Reactive Intermediate. *Organometallics* **2009**, *28*, 4452−4463.

(8) Plenio, H. The Coordination Chemistry of the CF Unit in Fluorocarbons. *Chem. Rev.* **1997**, *97*, 3363−3384.

(9) Romero, E. A.; Zhao, T.; Nakano, R.; Hu, X.; Wu, Y.; Jazzar, R.; Bertrand, G. Tandem Copper Hydride−Lewis Pair Catalysed Reduction of Carbon Dioxide into Formate with Dihydrogen. *Nat. Catal.* **2018**, *1*, 743−747.

(10) Cotton, F. A.; Dikarev, E. V.; Petrukhina, M. A. Syntheses and Crystal Structures of "Unligated" Copper(I) and Copper(II) Trifluoroacetates. *Inorg. Chem.* **2000**, *39*, 6072−6079.

(11) Fisher, K. J.; Materna, K. L.; Mercado, B. Q.; Crabtree, R. H.; Brudvig, G. W. Electrocatalytic Water Oxidation by a Copper(II) Complex of an Oxidation-Resistant Ligand. *ACS Catal.* **2017**, *7*, 3384−3387.

(12) Mukherjee, R. Copper. In *Comprehensive Coordination Chemistry II: From Biology to Nanotechnology*; McCleverty, J. A., Meyer, T. J., Fenton, D. E., Eds.; Elsevier/Pergamon: 2004; Vol. *6*, pp 747−910. DOI: 10.1016/B0-08-043748-6/90010-0.
(13) Ye, S.; Sarkar, B.; Lissner, F.; Schleid, T.; Van Slageren, J.; Fiedler, J.; Kaim, W. Three-Spin System with a Twist: A Bis(Semiquinonato)Copper Complex with a Nonplanar Configuration at the Copper(II) Center. *Angew. Chem., Int. Ed.* **2005**, *44*, 2103−2106.
(14) Flores, J. A.; Andino, J. G.; Lord, R. L.; Wolfe, R. J.; Park, H.; Pink, M.; Telser, J.; Caulton, K. G. Probing Redox Noninnocence of Copper and Zinc Bis-Pyridylpyrrolides. *Eur. J. Inorg. Chem.* **2018**, *2018*, 4893−4904.
(15) Kasumov, V. T.; Süzergöz, F.; Sahin, E.; Çelik, Ö.; Aslanoğlu, M. Synthesis, Characterization and Effect of the Fluorine Substitution on the Redox Reactivity and in Vitro Anticancer Behaviors of N-Polyfluorophenyl-3,5-Di- Tert-Butylsalicylaldimines and Their Cu(II) Complexes. *J. Fluorine Chem.* **2014**, *162*, 78−89.
(16) Pereira, M. B.; Fontana, L. A.; Siqueira, J. D.; Auras, B. L.; da Silva, M. P.; Neves, A.; Gabriel, P.; Terenzi, H.; Iglesias, B. A.; Back, D. F. Pyridoxal Derivatized Copper(II) Complexes: Evaluation of Antioxidant, Catecholase, and DNA Cleavage Activity. *Inorg. Chim. Acta* **2018**, *469*, 561−575.
(17) Cordero, B.; Gómez, V.; Platero-Prats, A. E.; Revés, M.; Echeverría, J.; Cremades, E.; Barragán, F.; Alvarez, S. Covalent Radii Revisited. *Dalton Trans.* **2008**, *21*, 2832−2838.
(18) Bondi, A. Van Der Waals Volumes and Radii. *J. Phys. Chem.* **1964**, *68*, 441−451.
(19) Yokoi, H.; Addison, A. W. Spectroscopic and Redox Properties of Pseudotetrahedral Copper(II) Complexes. Their Relationship to Copper Proteins. *Inorg. Chem.* **1977**, *16*, 1341−1349.
(20) Stanek, K.; Czarniecki, B.; Aardoom, R.; Rüegger, H.; Togni, A. Remote C-F-Metal Interactions in Late-Transition-Metal Complexes. *Organometallics* **2010**, *29*, 2540−2546.
(21) Skeel, B. A.; Boreen, M. A.; Lohrey, T. D.; Arnold, J. Perturbation of $^{1}J_{C,F}$ Coupling in Carbon-Fluorine Bonds on Coordination to Lewis Acids: A Structural, Spectroscopic, and Computational Study. *Inorg. Chem.* **2020**, *59*, 17259−17267.
(22) Lee, C.; Yang, W.; Parr, R. G. Development of the Colle-Salvetti Correlation-Energy Formula into a Functional of the Electron Density. *Phys. Rev. B: Condens. Matter Mater. Phys.* **1988**, *37*, 785−789.
(23) Becke, A. D. Density-Functional Thermochemistry. III. The Role of Exact Exchange. *J. Chem. Phys.* **1993**, *98*, 5648−5652.
(24) Hehre, W. J.; Ditchfield, R.; Pople, J. A. Self-Consistent Molecular Orbital Methods. XII. Further Extensions of Gaussian-Type Basis Sets for Use in Molecular Orbital Studies of Organic Molecules. *J. Chem. Phys.* **1972**, *56*, 2257−2261.
(25) Hariharan, P. C.; Pople, J. A. The Influence of Polarization Functions on Molecular Orbital Hydrogenation Energies. *Theor. Chim. Acta* **1973**, *28*, 213−222.
(26) Clark, T.; Chandrasekhar, J.; Spitznagel, G. W.; Schleyer, P. V. R. Efficient Diffuse Function-Augmented Basis Sets for Anion Calculations. III. The 3-21+G Basis Set for First-Row Elements, Li-F. *J. Comput. Chem.* **1983**, *4*, 294−301.
(27) Francl, M. M.; Pietro, W. J.; Hehre, W. J.; Binkley, J. S.; Gordon, M. S.; DeFrees, D. J.; Pople, J. A. Self-Consistent Molecular Orbital Methods. XXIII. A Polarization-Type Basis Set for Second-Row Elements. *J. Chem. Phys.* **1982**, *77*, 3654−3665.
(28) Rassolov, V. A.; Pople, J. A.; Ratner, M. A.; Windus, T. L. 6-31G* Basis Set for Atoms K through Zn. *J. Chem. Phys.* **1998**, *109*, 1223−1229.
(29) Frisch, M. J.; Trucks, G. W.; Schlegel, H. B.; Scuseria, G. E.; Robb, M. A.; Cheeseman, J. R.; Scalmani, G.; Barone, V.; Petersson, G. A.; Nakatsuji, H.; et al. *Gaussian 16, Rev. C.01*; Gaussian Inc.: 2016.
(30) Krishnan, R.; Binkley, J. S.; Seeger, R.; Pople, J. A. Self-Consistent Molecular Orbital Methods. XX. A Basis Set for Correlated Wave Functions. *J. Chem. Phys.* **1980**, *72*, 650−654.
(31) McLean, A. D.; Chandler, G. S. Contracted Gaussian Basis Sets for Molecular Calculations. I. Second Row Atoms, Z = 11−18. *J. Chem. Phys.* **1980**, *72*, 5639−5648.
(32) Wachters, A. J. H. Gaussian Basis Set for Molecular Wavefunctions Containing Third-Row Atoms. *J. Chem. Phys.* **1970**, *52*, 1033−1036.
(33) Hay, P. J. Gaussian Basis Sets for Molecular Calculations. The Representation of 3d Orbitals in Transition-Metal Atoms. *J. Chem. Phys.* **1977**, *66*, 4377−4384.
(34) Raghavachari, K.; Trucks, G. W. Highly Correlated Systems. Excitation Energies of First Row Transition Metals Sc-Cu. *J. Chem. Phys.* **1989**, *91*, 1062−1065.
(35) Frisch, M. J.; Pople, J. A.; Binkley, J. S. Self-Consistent Molecular Orbital Methods 25. Supplementary Functions for Gaussian Basis Sets. *J. Chem. Phys.* **1984**, *80*, 3265−3269.
(36) Marenich, A. V.; Cramer, C. J.; Truhlar, D. G. Universal Solvation Model Based on Solute Electron Density and on a Continuum Model of the Solvent Defined by the Bulk Dielectric Constant and Atomic Surface Tensions. *J. Phys. Chem. B* **2009**, *113*, 6378−6396.
(37) Glendening, E. D.; Reed, A. E.; Carpenter, J. E.; Weinhold, F. *NBO, Ver. 3.1*; University of Wisconsin: 2016.
(38) Foster, J. P.; Weinhold, F. Natural Hybrid Orbitals. *J. Am. Chem. Soc.* **1980**, *102*, 7211−7218.
(39) Bader, R. F. W. *Atoms in Molecules: A Quantum Theory*; Oxford University Press: 1990.
(40) Lu, T.; Chen, F. Multiwfn: A Multifunctional Wavefunction Analyzer. *J. Comput. Chem.* **2012**, *33*, 580−592.
(41) Mountain, A. R. E.; Kaltsoyannis, N. Do QTAIM Metrics Correlate with the Strength of Heavy Element-Ligand Bonds? *Dalton Trans.* **2013**, *42*, 13477−13486.
(42) Firme, C. L.; Antunes, O. A. C.; Esteves, P. M. Relation between Bond Order and Delocalization Index of QTAIM. *Chem. Phys. Lett.* **2009**, *468*, 129−133.
(43) Yang, L.; Powell, D. R.; Houser, R. P. Structural Variation in Copper(I) Complexes with Pyridylmethylamide Ligands: Structural Analysis with a New Four-Coordinate Geometry Index, τ_4. *Dalton Trans.* **2007**, 955−964.
(44) Echeverría, J.; Cremades, E.; Amoroso, A. J.; Alvarez, S. Jahn-Teller Distortions of Six-Coordinate Cu(II) Compounds: Cis or Trans? *Chem. Commun.* **2009**, 4242−4244.

https://doi.org/10.1021/acs.inorgchem.1c01958
Inorg. Chem. 2021, 60, 14759−14764